Annals of Nuclear Cardiology Vol. 4 No. 1 155−162

REVIEW ARTICLE—JSNC AWARD

Nuclear Molecular Imaging of the Failing Heart: Evaluation of Cardiac Sympathetic Nerve Activity and Mitochondrial Function in Patients with Cardiomyopathy

Satoru Ohshima, MD, PhD[1), 2), 3)], Satoshi Isobe, MD, PhD[3)] and Toyoaki Murohara, MD, PhD[3)]

Received: August 6, 2016/Revised manuscript received: September 1, 2017/Accepted: September 20, 2017
J-STAGE Advance published: July 23, 2018

Abstract

Nuclear imaging of failing myocardium is targeting the impaired part related to several processes of myocardial metabolism or work. Myocardium mainly utilizes fatty acid or glucose for ATP production in mitochondria. Intracellular calcium handling, which needs an amount of ATPs, induces myocardial contraction and relaxation, and is regulated with beta adrenal-stimulation. In the failing myocardium, any of these parts related to the myocardial work are variedly impaired, and could be the imaging target. Despite recent advancement of heart failure treatment, the patients with heart failure remain in high morbidity and mortality. For appropriate managements or prediction of prognosis in patients with heart failure, it is important to evaluate the mechanism of the failing myocardium. In this article, we focus on the usefulness of the 2 radionuclide imaging in evaluating sympathetic nerve function using myocardial ^{123}I-MIBG scintigraphy and mitochondrial function using myocardial ^{99m}Tc-sestamibi SPECT in the patients with cardiomyopathy.

Keywords: Cardiomyopathy, Failing myocardium, Heart failure, Mitochondria, Sestamibi, Sympathetic nerve
Ann Nucl Cardiol 2018；4（1）：155−162

Nuclear imaging of the failing myocardium is targeting the impaired part related to several processes of myocardial metabolism or work. Myocardium mainly utilizes fatty acid or glucose as the energy source in the aerobic metabolism to produce adenosine triphosphate (ATP), and each of them is targeted as ^{18}F-fludeoxyglucose (FDG) - positron emission tomography (PET), ^{123}I-beta-methyl-p-iodophenyl pentadecanoic acid (BMIPP) (1, 2), or ^{11}C-Acetate PET (3). ATP production is made with oxidative regeneration in the mitochondria, and the mitochondrial function is visualized with ^{99m}Tc-sestamibi (4, 5), as described in detail later. Intracellular calcium handling, that needs an amount of ATPs in several processes, induces myocardial contraction and relaxation. Beta adrenal-stimulus by sympathetic nerve in the myocardium regulates the intracellular calcium handling, and is imaged with ^{123}I-metaiodobenzilguanidine (MIBG) (6) or ^{11}C-meta-hyroxyepedrine (HED) (7).

Despite recent advancement in heart failure treatment, patients with heart failure still remain in high morbidity and mortality rate (8). Heart failure is defined as the decompensated status of the hemodynamics with insufficient blood supply to peripheral tissues, not only due to low cardiac output caused by reduced myocardial contraction, but also due to the impairment of myocardial relaxation and stiffness, increased vessel resistance, or systemic fluid unbalance. Even if cardiac function is preserved at rest, the impairment of myocardial relaxation in left ventricular hypertrophy (9), or the reduced myocardial functional reserve in myocardial contraction or

doi: 10.17996/anc.18-00001

1) Satoru Ohshima
Department of Cardiology, Nagoya Kyoritsu Hospital, 1-172 Hokke, Nakagawa, Nagoya, Aichi 454-0933, Japan
2) Satoru Ohshima
Department of Cardiovascular Nuclear Imaging Center, Nagoya Radiological Diagnostic Foundation, 1−162 Hokke, Nakagawa, Nagoya, Aichi 454-0933, Japan
E-mail: kaku@nagoya-pet. or.jp
3) Satoru Ohshima, Satoshi Isobe, Toyoaki Murohara
Department of Cardiology, Nagoya University Graduate School of Medicine, 65 Tsurumai, Showa, Nagoya, Aichi 466-0065, Japan

relaxation at physical or pharmacological stress (10, 11) could cause heart failure. Accordingly, detailed evaluation of the myocardial properties in failing heart is important for appropriate treatments or the prediction of the prognosis in the patients with heart failure, using non-invasive imaging modalities, such as echocardiography, nuclear imaging, magnetic resonance image (MRI), or computed tomography (CT) (12-14).

In this article we focus on the clinical usefulness of the 2 radionuclide molecular imaging in evaluating myocardial mitochondrial function which produce myocardial energy source of ATPs using ^{99m}Tc-sestamibi, and the sympathetic nerve function which regulates the myocardial intracellular calcium handling in myocardial contraction and relaxation using ^{123}I-MIBG in patients with non- ischemic cardiomyopathy.

Sympathetic nerve functional imaging with ^{123}I-MIBG

Myocardial imaging with ^{123}I-MIBG, the analogue of norepinephrine (NE), could visualize the activity and the innervation of adrenal sympathetic nervous system in the heart, and is widely used for evaluation of the patients with heart failure (6, 15). Increased sympathetic nervous activity or denervation are seen in heart failure patients, and could be imaged with myocardial ^{123}I-MIBG image (16). Several reports have shown the clinical usefulness of ^{123}I-MIBG for prediction of major cardiac events, including heart failure hospitalization or cardiac death (17-20), discharge of implantable cardioverter defibrillator (21), or evaluation of the effectiveness of beta-blockade (22-26), renin-angiotensin-aldosterone system inhibitor (27-29), and nicorandil (30, 31) in patients with heart failure. And, a multi-center study of ADMIRE-HF (AdreView Myocardial Imaging for Risk Evaluation in Heart Failure) trial was conducted (32), and meta-analysis of Japanese-single cohort was also performed (33) and verified the perceptions of the previous studies. Myocardial ^{123}I-MIBG imaging is accepted as class I in the guideline of clinical use of nuclear medicine for patients with heart failure according to the Japanese Circulation Society (34).

On the other hand, reduced myocardial functional reserve during atrial pacing tachycardia or during dobutamine stress test is reportedly caused by the impairment of intracellular calcium handling, especially of SERCA2 or phospholamban (35-37) in the failing heart; and that is related to the poor prognosis (11, 38). We therefore investigated the relationship between the parameters of myocardial ^{123}I-MIBG imaging, myocardial functional reserve during atrial pacing stress or dobutamine stress, and mRNA gene expression of the protein related to calcium handling or beta-adrenal signaling in myocardial tissue in patients with idiopathic dilated cardiomyopathy (DCM) and hypertrophic cardiomyopathy (HCM).

We reported that patients with reduced delayed heart to mediastinum ratio (HMR) showed an impairment in myocardial functional reserve with reduced mRNA expressions of sarcoplasmic reticulum calcium ATPase (SERCA2a) and phospholamban during atrial pacing tachycardia in 24 DCM patients (39). And we demonstrated significant correlations between the washout rate or delayed HMR and myocardial functional reserve in DCM patients during dobutamine stress (40, 41) (Fig. 1 and 2). These parameters were also associated with mRNA expressions of the proteins related to calcium handling or beta-adrenal signaling. And we also demonstrated that ^{123}I-MIBG parameters are associated with impaired myocardial functional reserve during atrial pacing tachycardia in 30 HCM patients (42). In these studies, we showed that myocardial ^{123}I-MIBG imaging parameters could predict abnormal myocardial functional reserve related to the impairment of calcium handling or beta adrenal signaling in non-ischemic cardiomyopathy patients.

Mitochondrial functional imaging with ^{99m}Tc-Sestamibi

Myocardial mitochondria produce about 30 kg/day of ATPs as a myocardial energy source (43). Intra-mitochondrial membrane potential is strongly negative charged of -161 ± 7 mV in normal myocyte (44). When cardiomyocytes are damaged by myocardial ischemia or other causes, the mitochondrial membrane potential is increasing (45). ^{99m}Tc-sestamibi, which is generally used as the tracer of SPECT-MPI, is a mono-positive ion, and usually retained within the mitochondria by the strong negative membrane potential (46). However in the damaged myocyte with increased mitochondrial membrane potential, ^{99m}Tc-sestamibi is washed out from myocyte (47).

It is reported that mitochondria in large clusters varied in size and shape with few myofibrils in myocardial tissue of DCM patients (48). Also, it is reported that mitochondrial damages were seen in several other heart diseases (43). In experimental studies, increased washouts of ^{99m}Tc-sestamibi were seen in the model of myocardial ischemia and reperfusion (49), hypertensive heart failure (50), and pharmacological mitochondrial injury, related to mitochondrial damage (51). Several clinical investigations have also demonstrated the increased washout of ^{99m}Tc-sestamibi in patients with myocardial infarction with reperfusion (52, 53), severe ischemia with triple vessel disease (54), non-ischemic cardiomyopathy (4, 55, 56), mitochondrial cardiomyopathy (57), and post-chemotherapy cardiomyopathy (58).

We similarly investigated the relationship between the washout of ^{99m}Tc-sestamibi and the myocardial functional reserve of force frequency relation in patients with non-ischemic cardiomyopathy. We demonstrated that the washout rate of ^{99m}Tc-seatamibi was associated with myocardial

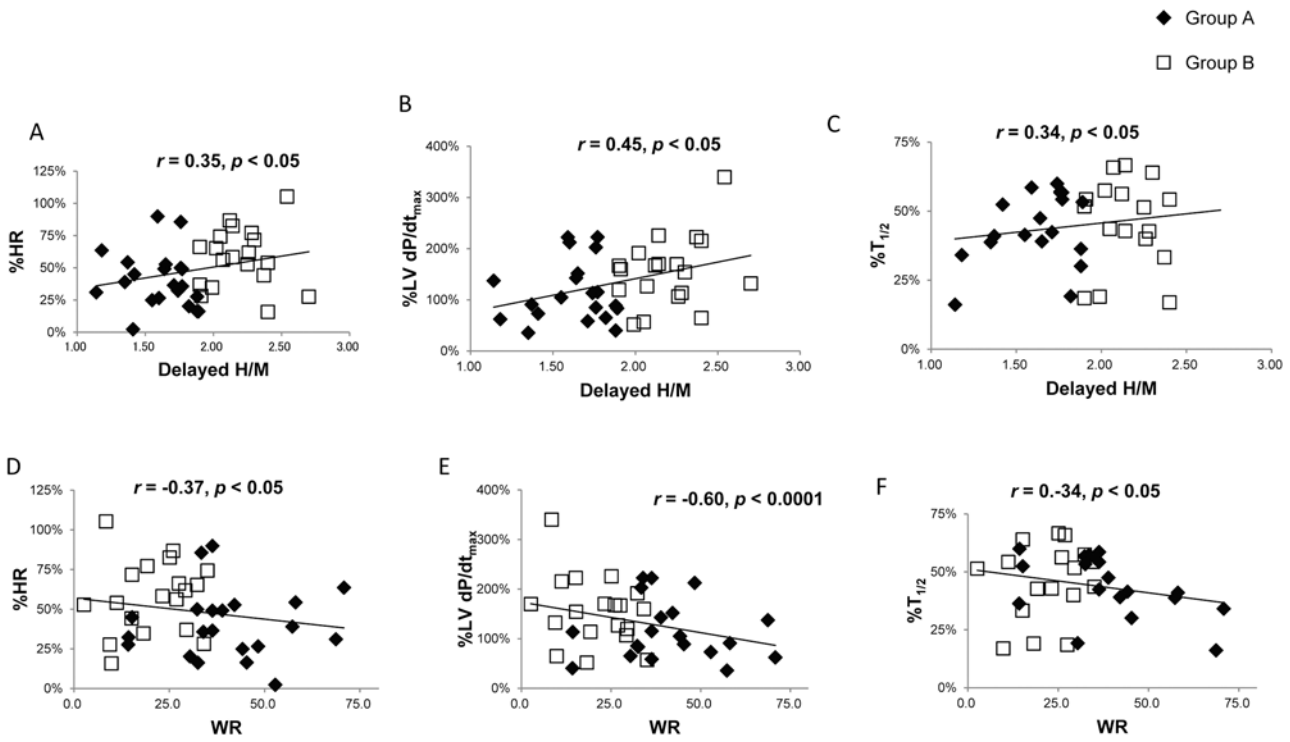

Fig. 1 Myocardial ^{123}I-MIBG in DCM patients.

A-C. Relationships between delayed H/M of ^{123}I-MIBG and the parameters of cardiac catheterization. Significant correlations were observed between delayed H/M and %HR (A), %LV dP/dt$_{max}$ (B), and %T$_{1/2}$ (C). Group A comprise the patients showing a delayed H/M ratio of <1.9 (median value). Group B comprise the patients showing that of ≥1.9.

D-F. Relationships between washout rate of ^{123}I-MIBG and parameters of cardiac catheterization. Significant correlations were observed between washout rate and %HR (D), %LV dP/dt$_{max}$ (E), and %T$_{1/2}$ (F). (From ref. (41) reprinted with permission.)

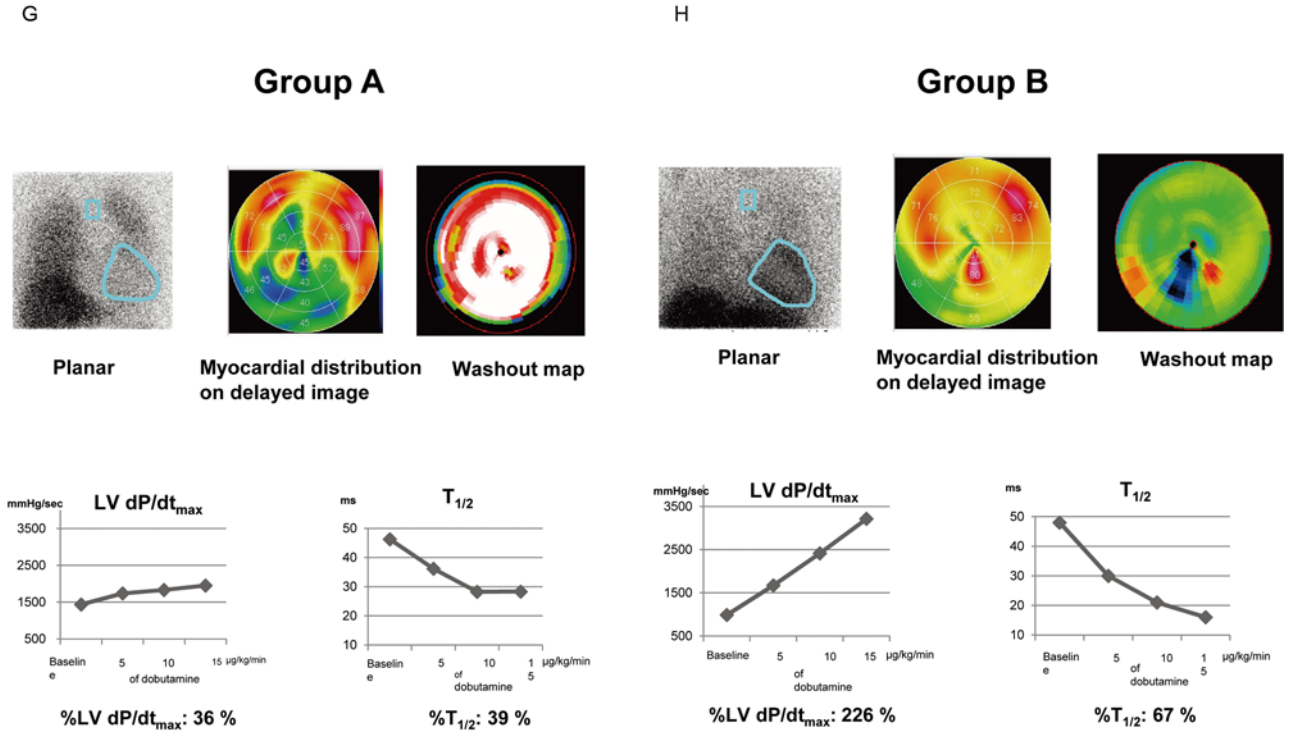

Fig. 2 Representative case of DCM patients in ^{123}I-MIBG study.

G. Representative case of group A. A patient with markedly reduced cardiac uptake (delayed H/M=1.5), globally increased washout of ^{123}I-MIBG shows impaired inotropic, chronotropic, and lusitropic responses to dobutamine stress.

H. Representative case of group B. A patient with preserved cardiac uptake (delayed H/M=2.3) and only slight washout in the inferior wall of ^{123}I-MIBG shows a favorable change in HR and fair inotropic and lusitropic responses to dobutamine stress. (From ref. (41) reprinted with permission.)

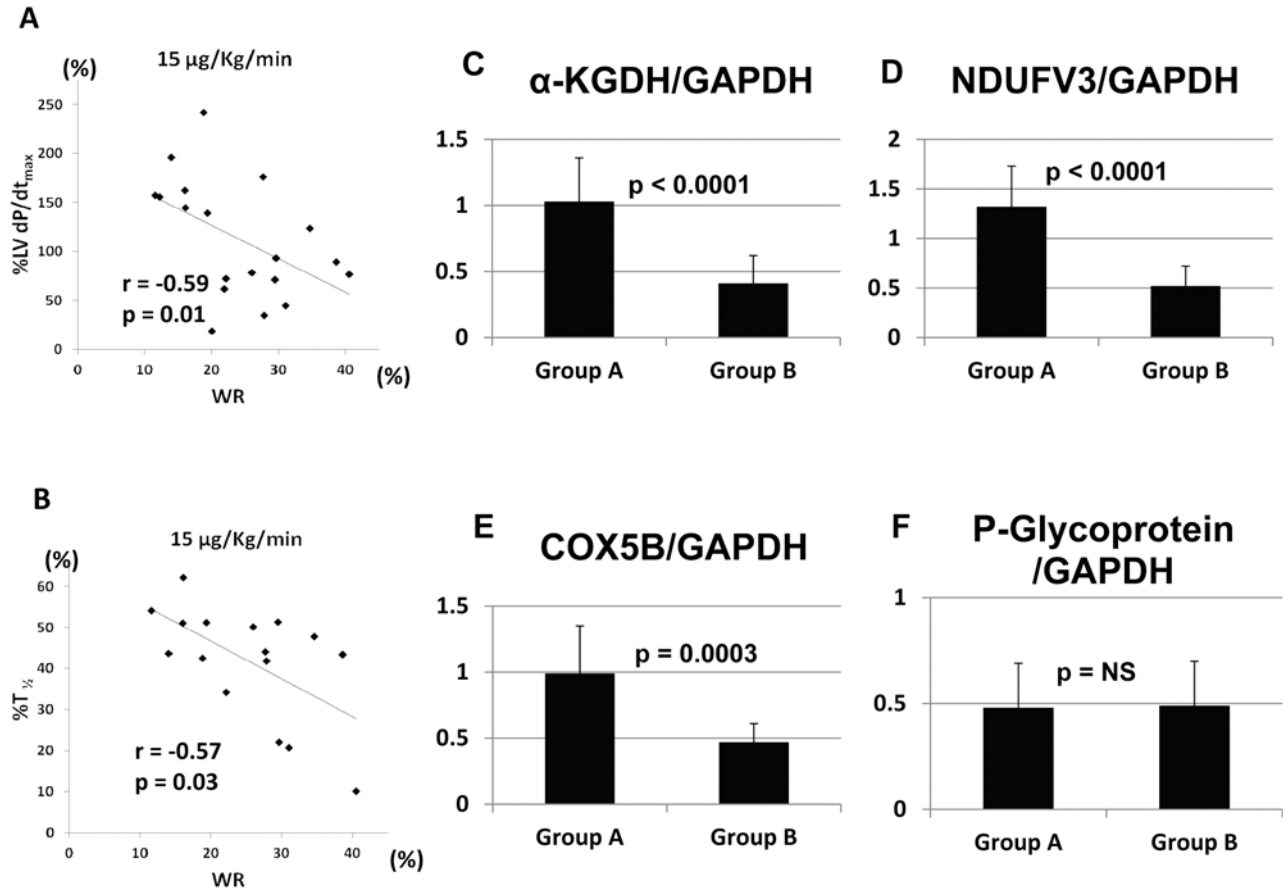

Fig. 3 ^{99m}Tc-sestamibi in DCM.

A, B. Relationship between ^{99m}Tc-sestamibi washout rate (WR) and hemodynamic changes from baseline to peak dobutamine stress. A. A significant inverse correlation was observed between ^{99m}Tc-sestamibi WR and % changes in LV dP/dt_{max} from baseline to peak (15 μg/kg/min) dobutamine stress. B. A significant inverse correlation was observed between ^{99m}Tc-sestamibi WR and % changes in $T_{1/2}$ from baseline to peak (15 μg/kg/min) dobutamine stress. C-F. Comparison of mitochondrial mRNA expression between the 2 Groups. α-KGDH (C), NDUFV3 (D), and COX5B (E) were significantly lower in Group B (WR of ^{99m}Tc-sestamibi ≤24.3%) than in Group A (WR of ^{99m}Tc-sestamibi >24.3%). The normal value of ^{99m}Tc-sestamibi washout rate of the age-matched control group (10 subject; 9 men; age: 56 ± 9 years) was 11 ± 5%. (From ref. (59) reprinted with permission.)

functional reserve during dobutamine stress, mitochondrial morphological and functional abnormalities in 20 DCM patients (59). DCM patients with increased washout of ^{99m}Tc-sestamibi showed reduced mRNA expressions of the proteins related to the mitochondrial electron transport chain, including α-KGDH, NDUFV3, and COX5B (Fig. 3). Significant correlations were observed between the washout rate of ^{99m}Tc-sestamibi and mitochondrial morphological abnormalities, as shown in abnormal mitochondrial shape and size, degeneration of the cristae formation, and the presence of glycogen positive area which represents an impairment in glucose utilization. Representative cases of each group are shown in Fig. 4. In 30 HCM patients, the increased washout of ^{99m}Tc-sestamibi was also related with the impairment force frequency relations during atrial pacing stress, and with mitochondrial functional damage of the protein related to electron transport, morphological abnormality of mitochondria as shown in disorganization or variation in size and increased number of mitochondria (60, 61).

Clinical implications

Myocardial mitochondria produce ATP to maintain myocardial function (43). Myocardial contraction and relaxation are caused by the sliding of actin and myosin filaments with intracellular calcium handling, which needs an amount of ATPs in several processes (Fig. 5) (62, 63). When myocardial mitochondria are impaired, these processes do not work well, leading to cardiac functional deterioration (64). Beta adrenal stimulus initiates and regulates the calcium handling process. The downregulation of beta receptors in the failing myocardium impairs several processes of intracellular calcium handling related to myocardial work. Consequently, it is important to figure out the pathogenesis of the failing heart with regard to sympathetic nervous system, mitochondrial function, calcium handling, or beta-adrenal signaling using myocardial ^{99m}Tc-sestamibi or ^{123}I-MIBG imaging.

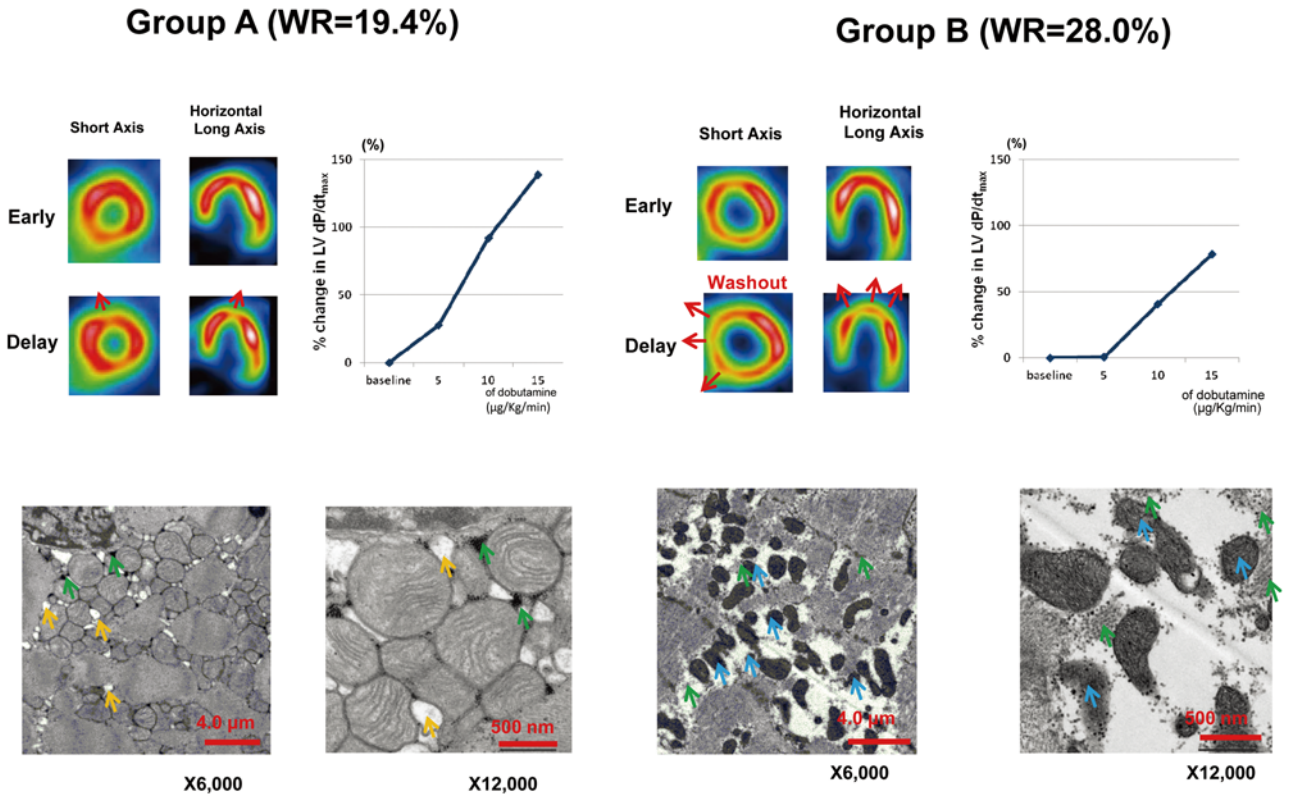

Fig. 4 Representative case of DCM patients in ^{99m}Tc-sestamibi study.

Representative Case of group A (Left). A 66-year-old man shows no global increased ^{99m}Tc-sestamibi WR (19.4%). An increased washout was observed in the small anteroseptal area (red arrows) on SPECT image. The %LV dP/dt$_{max}$ was favorably increased. Electron microscopy revealed a relatively preserved mitochondrial configuration as well as a small amount of glycogen accumulations (green arrows) and lipid droplets (yellow arrows).

Representative case of group B (Right). A 45-year-old woman exhibited an increased MIBI WR (28.3%). An increased washout was observed in the anteroseptal to the inferoseptal wall. The %LV dP/dt$_{max}$ showed a subtle increase in response to dobutamine. Electron microscopy reveals many damaged mitochondria (blue arrows) and glycogen accumulations (green arrows). (From ref. (59) reprinted with permission.)

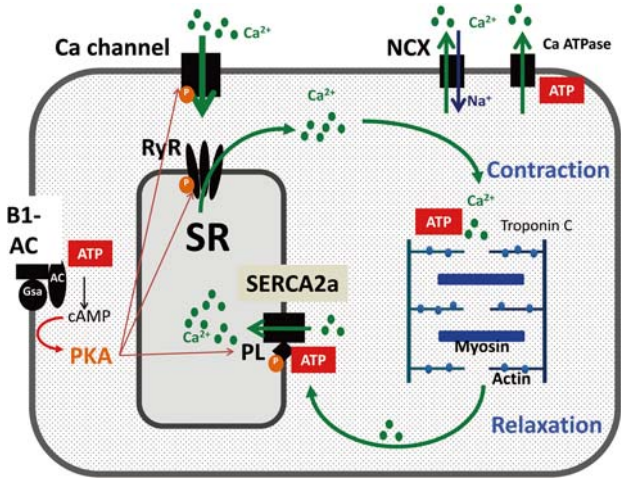

Fig. 5 Molecular mechanism of myocardial contraction and relaxation: intracellular calcium handling regulated with beta adrenergic signaling.

Calcium influx through cell membrane calcium channel induces calcium-induced calcium release from sarcoplasmic reticulum (SR) through ryanosine receptor (RyR). Then, intra-cellular calcium binding to the actin filament induces the sliding of the actin-myosin filament, resulting in myocardial contraction. Calcium dissociation from actin filament causes myocardial relaxation, and calcium is retaken up to SR through sarcoplasmic reticulum calcium ATPase (SERCA2a), regulated by phospholamban (PL). Intracellular calcium concentration is regulated with a calcium pump out through natrium calcium exchanger or plasma membrane calcium ATPase. Beta adrenal stimulus activates phosphokinase A, which makes for phosphorylation of calcium channel, RyR, PL, and the calcium handling cycle is activated. Each process consumes an amount of ATP, and the lack of ATP would have a harmful effect on calcium handling and reduced cardiac function.

NCX: Na^+/Ca^{2+} exchanger, SR: sarcoplasmic reticulum; SERCA2: sarcoplasmic reticulum Ca^{2+} ATPase, PL: phospholamban, PKA: phosphokinase A, CAMP: cyclic AMP, AC: adenylate cyclase, RyR: Ryanosine receptor, B1-AR: beta1 adrenal-receptor. (From ref. (63) reprinted with permission.)

And previously described, the parameter of myocardial ^{123}I-MIBG and ^{99m}Tc-sestamibi scintigraphy could predict the poor prognosis, select the responder of the pharmacological or device treatment, or could be used the evaluation of the effectiveness of the various treatments in the patients with various heart disease, including ischemic heart disease or cardiomyopathies. And the combined evaluations of these molecular parameters with the other non-invasive imaging modalities could make appropriate management for favorable prognosis in heart failure patients.

Conclusions

The myocardial imaging with ^{99m}Tc-sestamibi and ^{123}I-MIBG could visualize myocardial mitochondrial or sympathetic nervous function, that is closely related to myocardial work at the molecular level. These radionuclide imaging contribute to make for a profound understanding of the essential mechanism of pathogenesis of the failing myocardium.

Acknowledgments

We are gratefully to Drs. Kazumasa Unno and Daisuke Hayashi for their great contribution to this work.

Sources of funding

None.

Conflict of interests

The authors have no conflict of interests with the work presented in this manuscript.

Abbreviations and Acronyms
BMIPP: Beta-methyl-p-iodophenyl pentadecanoic acid
DCM: Dilated cardiomyopathy
HCM: Hypertrophic cardiomyopathy
MIBG: Metaiodobenzilguanidine
MPI: Myocardial perfusion imaging
SPECT: Single-photon emission computed tomography

Reprint requests and correspondence:
Satoru Ohshima, MD, PhD
Department of Cardiology, Nagoya Kyoritsu Hospital, 1-172 Hokke, Nakagawa, Nagoya, Aichi 454-0933, Japan
E−mail: kaku@nagoya-pet.or.jp

References

1. Ishida Y, Yasumura Y, Nagaya N, et al. Myocardial imaging with ^{123}I-BMIPP in patients with congestive heart failure. Int J Card Imaging 1999; 15: 71-7.
2. Nishimura T. beta-Methyl-p-^{123}I-iodophenyl pentadecanoic acid single-photon emission computed tomography in cardiomyopathy. Int J Card Imaging 1999; 15: 41-8.
3. Naya M, Tamaki N. Imaging of Myocardial Oxidative Metabolism in Heart Failure. Curr Cardiovasc Imaging Rep 2014; 7: 9244.
4. Matsuo S, Nakae I, Tsutamoto T, et al. A novel clinical indicator using Tc-99m sestamibi for evaluating cardiac mitochondrial function in patients with cardiomyopathies. J Nucl Cardiol 2007; 14: 215-20.
5. Matsuo S, Nakajima K, Kinuya S. Clinical use of nuclear cardiology in the assessment of heart failure. World J Cardiol 2010; 2: 344-56.
6. Carrió I, Cowie MR, Yamazaki J, et al. Cardiac sympathetic imaging with mIBG in heart failure. JACC Cardiovasc Imaging 2010; 3: 92-100.
7. Boschi S, Lodi F, Boschi L, et al. 11C-meta-hydroxyephedrine: a promising PET radiopharmaceutical for imaging the sympathetic nervous system. Clin Nucl Med 2015; 40: e96-e103.
8. Roger VL, Weston SA, Redfield MM, et al. Trends in heart failure incidence and survival in a community-based population. JAMA 2004; 292: 344-50.
9. Hogg K, Swedberg K, McMurray J. Heart failure with preserved left ventricular systolic function; epidemiology, clinical characteristics, and prognosis. J Am Coll Cardiol 2004; 43: 317-27.
10. Kitaoka H, Takata J, Yabe T, et al. Low dose dobutamine stress echocardiography predicts the improvement of left ventricular systolic function in dilated cardiomyopathy. Heart 1999; 81: 523-7.
11. Scrutinio D, Napoli V, Passantino A, et al. Low-dose dobutamine responsiveness in idiopathic dilated cardiomyopathy: relation to exercise capacity and clinical outcome. Eur Heart J 2000; 21: 927-34.
12. Yancy CW, Jessup M, Bozkurt B, et al. 2013 ACCF/AHA guideline for the management of heart failure: a report of the American College of Cardiology Foundation/American Heart Association Task Force on Practice Guidelines. J Am Coll Cardiol 2013; 62: e147-239.
13. Carr JJ, Hendel RC, White RD, et al. 2013 appropriate utilization of cardiovascular imaging: a methodology for the development of joint criteria for the appropriate utilization of cardiovascular imaging by the American College of Cardiology Foundation and American College of Radiology. J Am Coll Radiol 2013; 10: 456-63.
14. White RD, Patel MR, Abbara S, et al. 2013 ACCF/ACR/ASE/ASNC/SCCT/SCMR appropriate utilization of cardiovascular imaging in heart failure: an executive summary: a joint report of the ACR Appropriateness Criteria® Committee and the ACCF Appropriate Use Criteria Task Force. J Am Coll Radiol 2013; 10: 493-500.
15. Wieland DM, Wu J, Brown LE, Mangner TJ, Swanson DP, Beierwaltes WH. Radiolabeled adrenergi neuron-blocking agents: adrenomedullary imaging with [131I] iodobenzylguanidine. J Nucl Med 1980; 21: 349-53.
16. Jessup M, Brozena S. Heart failure. N Engl J Med 2003; 348: 2007-18.
17. Merlet P, Valette H, Dubois-Randé JL, et al. Prognostic value of cardiac metaiodobenzylguanidine imaging in patients with heart failure. J Nucl Med 1992; 33: 471-7.

18. Kasama S, Toyama T, Sumino H, et al. Prognostic value of serial cardiac ^{123}I-MIBG imaging in patients with stabilized chronic heart failure and reduced left ventricular ejection fraction. J Nucl Med 2008; 49: 907-14.
19. Kasama S, Toyama T, Kurabayashi M. Serial ^{123}I-metaiodobenzylguanidine imaging predicts the risk of sudden cardiac death in patients with chronic heart failure. Int J Cardiol 2015; 179: 82-3.
20. Merlet P, Benvenuti C, Moyse D, et al. Prognostic value of MIBG imaging in idiopathic dilated cardiomyopathy. J Nucl Med 1999; 40: 917-23.
21. Boogers MJ, Borleffs CJ, Henneman MM, et al. Cardiac sympathetic denervation assessed with 123-iodine metaiodobenzylguanidine imaging predicts ventricular arrhythmias in implantable cardioverter-defibrillator patients. J Am Coll Cardiol 2010; 55: 2769-77.
22. Fukuoka S, Hayashida K, Hirose Y, et al. Use of iodine-123 metaiodobenzylguanidine myocardial imaging to predict the effectiveness of beta-blocker therapy in patients with dilated cardiomyopathy. Eur J Nucl Med 1997; 24: 523-9.
23. Kakuchi H, Sasaki T, Ishida Y, et al. Clinical usefulness of ^{123}I meta-iodobenzylguanidine imaging in predicting the effectiveness of beta blockers for patients with idiopathic dilated cardiomyopathy before and soon after treatment. Heart 1999; 81: 148-52.
24. Kasama S, Toyama T, Hatori T, et al. Evaluation of cardiac sympathetic nerve activity and left ventricular remodelling in patients with dilated cardiomyopathy on the treatment containing carvedilol. Eur Heart J 2007; 28: 989-95.
25. Fujimoto S, Inoue A, Hisatake S, et al. Usefulness of ^{123}I-metaiodobenzylguanidine myocardial scintigraphy for predicting the effectiveness of beta-blockers in patients with dilated cardiomyopathy from the standpoint of long-term prognosis. Eur J Nucl Med Mol Imaging 2004; 31: 1356-61.
26. Cohen-Solal A, Rouzet F, Berdeaux A, et al. Effects of carvedilol on myocardial sympathetic innervation in patients with chronic heart failure. J Nucl Med 2005; 46: 1796-803.
27. Kasama S, Toyama T, Kumakura H, et al. Addition of valsartan to an angiotensin-converting enzyme inhibitor improves cardiac sympathetic nerve activity and left ventricular function in patients with congestive heart failure. J Nucl Med 2003; 44: 884-90.
28. Kasama S, Toyama T, Hatori T, et al. Comparative effects of valsartan and enalapril on cardiac sympathetic nerve activity and plasma brain natriuretic peptide in patients with congestive heart failure. Heart 2006; 92: 625-30.
29. Kasama S, Toyama T, Kumakura H, et al. Spironolactone improves cardiac sympathetic nerve activity and symptoms in patients with congestive heart failure. J Nucl Med 2002; 43: 1279-85.
30. Kasama S, Toyama T, Kumakura H, et al. Effects of nicorandil on cardiac sympathetic nerve activity after reperfusion therapy in patients with first anterior acute myocardial infarction. Eur J Nucl Med Mol Imaging 2005; 32: 322-8.
31. Kasama S, Toyama T, Hatori T, et al. Comparative effects of nicorandil with isosorbide mononitrate on cardiac sympathetic nerve activity and left ventricular function in patients with ischemic cardiomyopathy. Am Heart J 2005; 150: 477.
32. Jacobson AF, Senior R, Cerqueira MD, et al. Myocardial iodine-123 meta-iodobenzylguanidine imaging and cardiac events in heart failure. Results of the prospective ADMIRE-HF (AdreView Myocardial Imaging for Risk Evaluation in Heart Failure) study. J Am Coll Cardiol 2010; 55: 2212-21.
33. Nakata T, Nakajima K, Yamashina S, et al. A pooled analysis of multicenter cohort studies of (123) I-mIBG imaging of sympathetic innervation for assessment of long-term prognosis in heart failure. JACC Cardiovasc Imaging 2013; 6: 772-84.
34. JCS Joint Working Group. Guidelines for clinical use of cardiac nuclear medicine (JCS 2010) -digest version-. Circ J 2012; 76: 761-7.
35. Feldman MD, Alderman JD, Aroesty JM, et al. Depression of systolic and diastolic myocardial reserve during atrial pacing tachycardia in patients with dilated cardiomyopathy. J Clin Invest 1988; 82: 1661-9.
36. Hasenfuss G, Holubarsch C, Hermann HP, et al. Influence of the force-frequency relationship on haemodynamics and left ventricular function in patients with non-failing hearts and in patients with dilated cardiomyopathy. Eur Heart J 1994; 15: 164-70.
37. Kim IS, Izawa H, Sobue T, et al. Prognostic value of mechanical efficiency in ambulatory patients with idiopathic dilated cardiomyopathy in sinus rhythm. J Am Coll Cardiol 2002; 39: 1264-8.
38. Nagaoka H, Isobe N, Kubota S, et al. Myocardial contractile reserve as prognostic determinant in patients with idiopathic dilated cardiomyopathy without overt heart failure. Chest 1997; 111: 344-50.
39. Ohshima S, Isobe S, Izawa H, et al. Cardiac sympathetic dysfunction correlates with abnormal myocardial contractile reserve in dilated cardiomyopathy patients. J Am Coll Cardiol 2005; 46: 2061-8.
40. Kobayashi M, Izawa H, Cheng XW, et al. Dobutamine stress testing as a diagnostic tool for evaluation of myocardial contractile reserve in asymptomatic or mildly symptomatic patients with dilated cardiomyopathy. JACC Cardiovasc Imaging 2008; 1: 718-26.
41. Ohshima S, Isobe S, Hayashi D, et al. Myocardial ^{123}I-MIBG scintigraphy predicts an impairment in myocardial functional reserve during dobutamine stress in patients with idiopathic dilated cardiomyopathy. Eur J Nucl Med Mol Imaging 2013; 40: 262-70.
42. Isobe S, Izawa H, Iwase M, et al. Cardiac ^{123}I-MIBG reflects left ventricular functional reserve in patients with nonobstructive hypertrophic cardiomyopathy. J Nucl Med 2005; 46: 909-16.
43. Murray AJ, Edwards LM, Clarke K. Mitochondria and heart failure. Curr Opin Clin Nutr Metab Care. 2007; 10: 704-11.
44. Chen LB. Mitochondrial membrane potential in living cells. Annu Rev Cell Biol 1988; 4: 155-81.
45. Konno N, Kako KJ. Effects of hydrogen peroxide and hypochlorite on membrane potential of mitochondria in situ in rat heart cells. Can J Physiol Pharmacol 1991; 69: 1705-12.
46. Carvalho PA, Chiu ML, Kronauge JF, et al. Subcellular distribution and analysis of technetium-99m-MIBI in isolated perfused rat hearts. J Nucl Med 1992; 33: 1516-22.
47. Piwnica-Worms D, Kronauge JF, Chiu ML. Uptake and retention of hexakis (2-methoxyisobutyl isonitrile) technetium (I) in cultured chick myocardial cells. Mitochondrial and

plasma membrane potential dependence. Circulation 1990; 82: 1826-38.
48. Schaper J, Froede R, Hein S, et al. Impairment of the myocardial ultrastructure and changes of the cytoskeleton in dilated cardiomyopathy. Circulation 1991; 83: 504-14.
49. Li QS, Frank TL, Franceschi D, et al. Technetium-99m methoxyisobutyl isonitrile (RP30) for quantification of myocardial ischemia and reperfusion in dogs. J Nucl Med 1988; 29: 1539-48.
50. Fukushima K, Momose M, Kondo C, et al. Myocardial ^{99m}Tc-sestamibi extraction and washout in hypertensive heart failure using an isolated rat heart. Nucl Med Biol 2010; 37: 1005-12.
51. Kawamoto A, Kato T, Shioi T, et al. Measurement of technetium-99m sestamibi signals in rats administered a mitochondrial uncoupler and in a rat model of heart failure. PLoS One 2015; 10: e0117091.
52. Takeishi Y, Sukekawa H, Fujiwara S, et al. Reverse redistribution of technetium-99m-sestamibi following direct PTCA in acute myocardial infarction. J Nucl Med 1996; 37: 1289-94.
53. Fujiwara S, Takeishi Y, Hirono O, et al. Reverse redistribution of ^{99m}Tc-sestamibi after direct percutaneous transluminal coronary angioplasty in acute myocardial infarction: relationship with wall motion and functional response to dobutamine stimulation. Nucl Med Commun 2001; 22: 1223-30.
54. Du B, Li N, Li X, et al. Myocardial washout rate of resting ^{99m}Tc-Sestamibi (MIBI) uptake to differentiate between normal perfusion and severe three-vessel coronary artery disease documented with invasive coronary angiography. Ann Nucl Med 2014; 28: 285-92.
55. Kumita S, Seino Y, Cho K, et al. Assessment of myocardial washout of Tc-99m-sestamibi in patients with chronic heart failure: comparison with normal control. Ann Nucl Med 2002; 16: 237-42.
56. Takehana K, Maeba H, Ueyama T, et al. Direct correlation between regional systolic function and regional washout rate of ^{99m}Tc-sestamibi in patients with idiopathic dilated cardiomyopathy. Nucl Med Commun 2011; 32: 1174-8.
57. Ikawa M, Kawai Y, Arakawa K, et al. Evaluation of respiratory chain failure in mitochondrial cardiomyopathy by assessments of ^{99m}Tc-MIBI washout and ^{123}I-BMIPP/^{99m}Tc-MIBI mismatch. Mitochondrion 2007; 7: 164-70.
58. Carboni GP. A novel clinical indicator using cardiac technetium-99m sestamibi kinetics for evaluating cardiotoxicity in cancer patients treated with multiagent chemotherapy. Am J Cardiovasc Dis. 2012; 2: 293-300.
59. Hayashi D, Ohshima S, Isobe S, et al. Increased ^{99m}Tc-sestamibi washout reflects impaired myocardial contractile and relaxation reserve during dobutamine stress due to mitochondrial dysfunction in dilated cardiomyopathy patients. J Am Coll Cardiol 2013; 61: 2007-17.
60. Unno K, Isobe S, Izawa H, et al. Relation of functional and morphological changes in mitochondria to myocardial contractile and relaxation reserves in asymptomatic to mildly symptomatic patients with hypertrophic cardiomyopathy. Eur Heart J 2009; 30: 1853-62.
61. Isobe S, Ohshima S, Unno K, et al. Relation of ^{99m}Tc-sestamibi washout with myocardial properties in patients with hypertrophic cardiomyopathy. J Nucl Cardiol 2010; 17: 1082-90.
62. Somura F, Izawa H, Iwase M, et al. Reduced myocardial sarcoplasmic reticulum Ca (2+)-ATPase mRNA expression and biphasic force-frequency relations in patients with hypertrophic cardiomyopathy. Circulation 2001; 104: 658-63.
63. Ohshima S, Isobe S, Murohara T. Molecular imaging of the failing heart: Assessment of cardiac sympathetic nerve and mitochondrial function. Int J Radiol Med Imag 2016; 2: 115-9.
64. Neubauer S. The failing heart — an engine out of fuel. N Engl J Med 2007; 356: 1140-51.